Jurnal Ilmiah Teknik Elektro Komputer dan Informatika (JITEKI)
Vol. 8, No. 2, June 2022, pp. 206-214
ISSN: 2338-3070, DOI: 10.26555/jiteki.v8i2.23622

Modeling and Analysis of Percentage Depth Dose (PDD) and Dose Profile of X-Ray Beam Produced by Linac Device with Voltage Variation

Bilalodin, Farzand Abdullatif
Department of Physics, Faculty of Mathematics and Natural Sciences, Jenderal Soedirman University, Purwokerto 53122, Indonesia

ARTICLE INFO

Article history:

Received March 20, 2022
Revised April 27, 2022
Accepted May 25, 2022

Keywords:

Modelling;
PDD;
Dose profile;
PHITS

ABSTRACT

The Percentage Depth Dose (PDD) and dose profile of X-Ray output from a LINAC therapy device has been modeled and analyzed. The research was conducted by simulation method through the use of the Particle and Heavy Ion Transport System (PHITS) program. The LINAC therapy device modeled in this work refers to the Siemens Primus LINAC therapy device, which is operated at 6 MV, 10 MV, and 18 MV voltages. Determination of PDD was carried at a depth of 0-30 cm and dose profile at a depth of 0-20 cm in a water phantom, placed at 100 cm from the source, which is exposed to a radiation field area of 10×10 cm^2. Results from the LINAC therapy device modeling agree with the actual X-ray apparatus and have produced Bremsstrahlung X-ray. The PDD curve analysis found that the maximum doses are at a depth of 1.5 cm, 2.5 cm, and 3.4 cm. The value of the build-up factor for each LINAC voltage agrees with the reference. Additionally, the results of the analysis of the dose profile suggest that the X-ray output has a good degree of uniformity. The flatness of the dose profile occurs at the depth of 20 cm with a percentage value of flatness at 1.6%, 1.9%, and 1.2%. The flatness values are all less than 2%. The flatness values show a $\leq$ 2% deviation from the reference value, which is below the tolerance range required in a measurement.

This work is licensed under a Creative Commons Attribution-Share Alike 4.0

Corresponding Author:

Bilalodin, Jenderal Soedirman University, Jl. dr. Soeparno Utara 61 Grendeng, Purwokerto 53122, Indonesia
Email: bilalodin@unsoed.ac.id

1. INTRODUCTION

Medical Linear Accelerator (LINAC) is an alternative therapy for cancer or tumors other than Cobalt 60 radiotherapy [1]. The main goal of LINAC radiotherapy is to provide a maximum dose to the tumor and a low dose to healthy cells near the tumor to improve quality of life and prolong patient survival [2]. In order to achieve this goal, the dose distribution produced by LINAC needs to be verified with an accurate method [3]. Two quantities that need to be verified before using the LINAC therapy device are the Percentage Depth Dose (PDD) and the dose profile [4][5].

Verification using a simulation approach is essential before LINAC therapy equipment is set up or prepared for the treatment of the patient [6]. One of the simulation methods to achieve this goal is the Monte Carlo method. The Monte Carlo method has been of great help in planning therapy using various radiation sources [7]. The method can also calculate in detail the spectral energy distribution of particles generated from the LINAC therapy apparatus as well as dosimetric calculations in the form of Percentage Depth Dose (PDD) and dose profiles [8].

Various Monte Carlo-based programs (codes) have been developed, such as MCNP, Geant4, and Penelope. MCNP is a Monte Carlo code developed by the Los Alamos National Laboratory. Geant4 was developed by CERN and KEK laboratories in 1993, and Francesc Salvat and colleagues developed Penelope at the University of Barcelona. In practice, the results vary due to differences in computational systems and in

nuclear data libraries included with the respective MC packages [9]. The weakness of the MCNP program is that it cannot visually display particle traces directly. On the other hand, Geant4 and Penelope are used only in the limited range of energy between 50 eV to 1 GeV [10].

The latest development is a code developed in Japan under Particle Heavy Ion Transport System (PHITS). The PHITS is a Monte Carlo method developed by the Japan Atomic Energy Agency (JAEA) to simulate nuclear processes in various research fields such as dosimetry, accelerator, shield design, space research, medical applications, and material research [11]. The advantage of the PHITS as a Monte Carlo-based program is that it is equipped with a tally that can visualize particle traces in 2 and 3 dimensions and calculate the physical quantity to be determined. The PHITS program is also suitable for simulating the transport of charged and uncharged particles that move randomly within the range of energy from 10^{-4} eV to 1 TeV [12].

The use of the PHITS program in this study contributes to a visual explanation of the mechanism of X-ray generation from the LINAC device and a more accurate determination of the PDD curve and dose profile. The accuracy in determining these parameters is a prerequisite before the LINAC device is used as a therapy instrument.

2. METHOD

The method used in this research is simulation. The research was conducted through several stages. The initial stage is literature and theoretical studies on the LINAC device, particularly the components that make up the LINAC head and important predetermined parameters before therapeutic operation. The following stage models the LINAC device by compiling the PHITS program input. The last stage is simulation to test the validity of the model and the determination of PDD parameters and dose profiles. The stages of the research are shown in Fig. 1.

Fig. 1. Flowchart of modeling and analysis of PDD and dose profile in the research

2.1. Modeling of LINAC Therapy Device

The modeling of the LINAC therapy device is focused on the LINAC head. This section is chosen because it is the place where X-ray is generated. The material composition used in modeling the LINAC head geometry is based on the Siemens Primus LINAC device. Only the main components of the LINAC head are modeled, namely the target, primary collimator, flattening filter, and secondary collimator [13]. The radiation field area used in this study is 10×10 cm^2 and the distance from Source to Skin Distance (SSD) is 100 cm [14]. The components that make up the LINAC head is shown in Table 1.

Table 1. Composition of the material components of the LINAC head [15]

LINAC Head Components	Materials	Percentage (%)	Density (g/cm^3)
Target	Tungsten (184W)	100	19.4
Primary Collimator	Tungsten (184W)	90.5	17
	Nickel (58Ni)	6.5	
	Iron (56Fe)	3	
Flattening Filter	Copper (63Cu)	69.17	8.92
	Copper (65Cu)	30.83	
Secondary Collimator	Tungsten (184W)	90.5	17
	Nickel (58Ni)	6.5	
	Iron (56Fe)	3	

The success of the X-ray head modeling is judged by the evidence of visualizing the traces of X-ray particles from escaping the target, passing through the components of the LINAC head, and penetrating the water phantom. Other evidence is the presence of an X-ray energy spectrum [16]. The geometry model of the LINAC head is shown in Fig. 2(a). The model of the LINAC head and visualization is shown in Fig. 2(b).

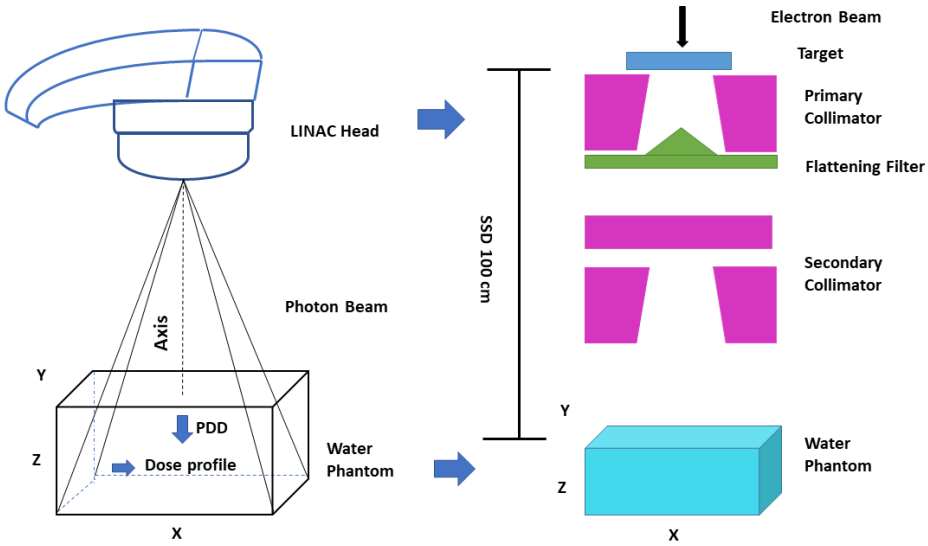

(a) (b)

Fig. 2. (a) Geometry of Linac head and water phantom. The x-ray photon beam emitted from the LINAC head is applied to the water phantom. PDD measurement in the direction of the Z-axis and the dose profile perpendicular to the direction of the beam (in the direction of the X-axis), (b) Model of the LINAC head and visualization of the components that make up the LINAC head based on the Simen Primus device

2.2. Determination of PDD Curve and Dose Profile

The standard water phantom determined the PPD curve and the dose profile of the X-ray radiation beam [17]. The water phantom is constructed as a cube of 40×40×40 cm^3 in size. In the phantom, a lattice of voxels (volumetric pixels) are made along the z and x axis. The voxels are designed as small cubes 1×1×1 cm^3 in size. The designed model of the water phantom interposed with voxels is shown in Fig. 3.

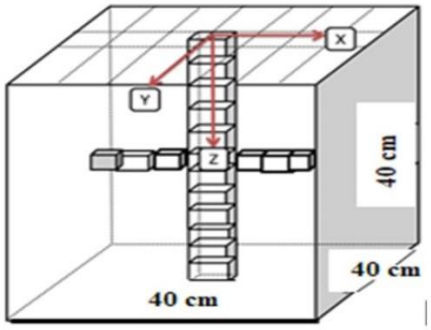

Fig. 3. Geometrical model of water phantom interposed with voxels for measurement of Percentage Depth Dose (PDD) and dose profile

The simulation to determine the PDD curve in the water phantom is carried out at a depth of 0 to 30 cm in the direction of the main axis (z-axis), while the dose profile is determined at a depth that ranges from 0 to 20 cm. The PDD values are calculated at every depth using Eq. (1) [18].

$$PDD = 100\frac{D_d}{D_{d0}} \quad (1)$$

with D_d is absorption dose at the depth d and D_{d0} is the maximum absorption dose.

Analysis on PDD and dose profile is carried out by finding the difference between the simulation results and the reference value. The stipulated difference is $\leq 2\%$. The flatness value is determined using Eq. (2) [19].

$$Flatness = 100\ \frac{D_{max} - D_{min}}{D_{min} + D_{max}} \quad (2)$$

with D_{max} is maximum dose and D_{min} is minimum dose.

The modeling of LINAC head and determination of PDD and dose profile use the PHITS program version 3.24. Visualization of trace particles and X-ray energy spectra uses the *tally tracks*. The determination of PDD values and dose profile, on the other hand, uses the *tally deposit*. The data library for the simulation uses cross sections from the JENDL-4.0 nuclear data library [12].

3. RESULTS AND DISCUSSION

3.1 Modeling The Geometry of LINAC Head

The results of the LINAC head geometry modeling using the PHITS program are shown in Fig. 4. The resulting model needs to be validated to ensure that the model truly represents the actual X-ray equipment. The criteria to ensure the head geometry model represents the actual equipment include the model being able to display the components of the LINAC head, the occurrence of X-rays from the target and their distribution, and the X-ray energy spectrum [16][20].

The high-energy electron beam interaction with the tungsten target produces X-ray radiation with a high-intensity value because tungsten is a target with a high atomic number. Targets with high atoms produce more X-ray radiation than targets with low atomic numbers [21][22].

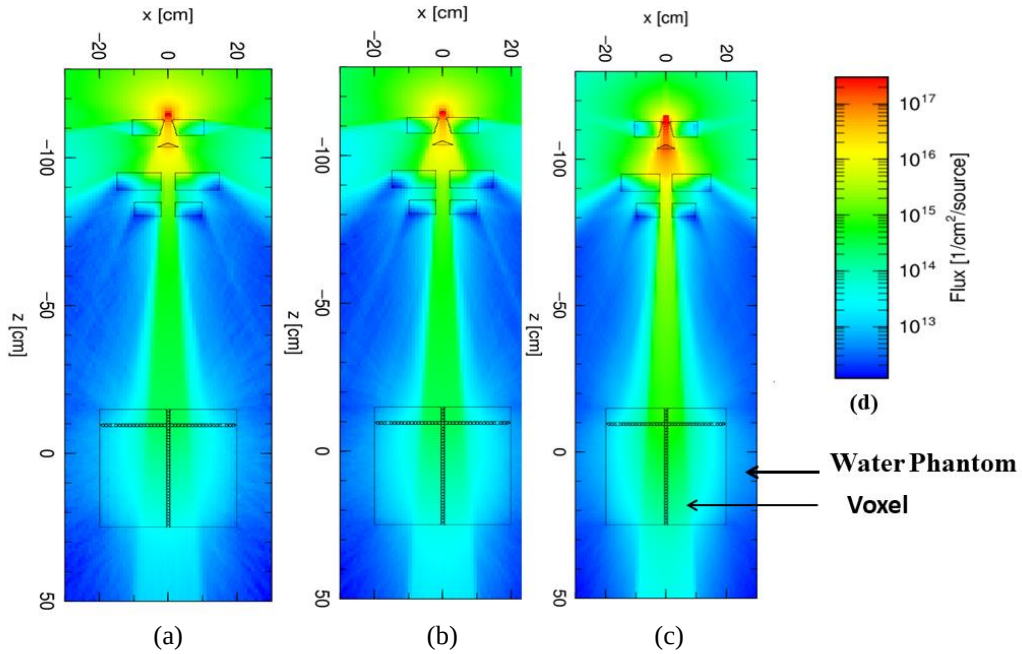

Fig. 4. Traces of X-ray particles produced by LINAC at working voltage of (a) 6 MV (b) 10 MV, and (c) 18 MV. The traces of X-ray particles resulting from the interaction of electrons with the target are depicted in color. Red represents high intensity, and blue represents low intensity, (d) The conversion of intensity in the flux value of X-ray photon

Fig. 3 also shows that the higher the LINAC voltage, the greater the X-ray intensity (shown by, the sharper red color). X-ray Photons generated from the target are passed through the primary collimator, flattening filter, secondary collimator, and water phantom. The X-ray intensity in the area around the target is 10^{16} (p/cm^2.s) and decreases in intensity when interacting with the primary collimator, flattening filter, and secondary collimator. The X-ray coming out of the secondary collimator decreases in intensity to 10^{15} (p/cm^2.s) and hit the water phantom with an intensity of 10^{14} (p/cm^{2}s).

The results of the X-ray spectrum from the modeling of the LINAC head are shown in Fig. 5. It can be seen that the X-ray intensity at the three different voltages of the LINAC forms a continuous spectrum. The continuous curve is called the bremsstrahlung curve [23]. The bremsstrahlung curve has maximum peak energy of 0.5 to 1.3 MeV. The maximum energy is generated through the pair production effect and X-rays interacting,

thus creating two annihilating photons, each having an energy of 0.51 MeV [24]. The results are in accordance with those obtained by Baumgartner et al. at the voltage of 10 and 18 MV [25].

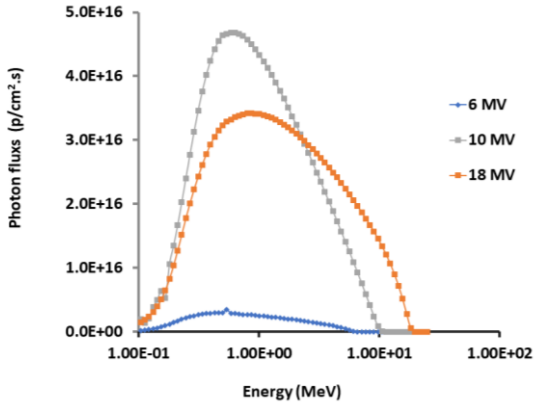

Fig. 5. X-Ray's energy spectrum at various LINAC working voltages**.** The X-axis represents energy, and the Y-axis represents the number of photon fluxes (X-ray intensity)

3.2 Percentage Depth Dose (PDD) and Dose Profile

3.2.1 Percentage Depth Dose (PDD)

PDD is an important parameter in studying the radiation dose distribution of X-ray photons along the main axis (*z*-axis) of LINAC. The calculation of PDD is carried out on the surface of the water phantom to a depth of 30 cm. The results of the PDD calculation are shown in Fig. 6, showing that the PDD curve of the three LINAC voltage variations appears to have a uniform graph trend. The PPD curve has a low surface dose pattern, then rises to a maximum value and decreases exponentially. The calculation results of the build-up value at 6, 10, and 18 MV voltages are found at a depth of 1.5 cm, 2.5 cm, and 3.4 cm, respectively.

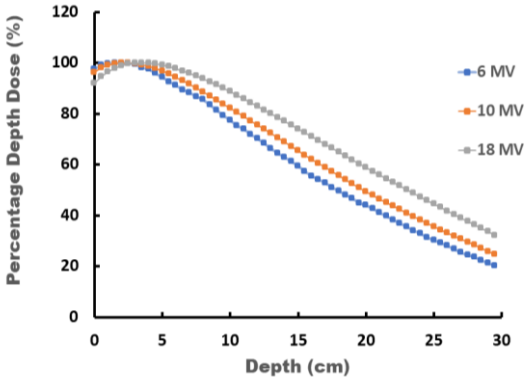

Fig. 6. PDD curve of the three LINAC voltage variations

The build-up value at voltages 6 and 10 MV corresponds to the reference, while 18 MV is smaller than the reference. The difference in the build-up value at 18 MV is 2%. This value is still within the allowable tolerance limit, which is $\leq$ 2% [26][27]. The maximum dose increases with the LINAC voltage, increasing the X-ray energy produced. X-ray photons can penetrate the water phantom deeper, so the build-up position is increasing [28][29].

3.2.2 Dose Profile

Dose profile refers to the relative dose distribution along the horizontal axis (*x*-axis) that is perpendicular to the direction of the incident X-ray radiation beam. The profile curve of radiation dose for each variation of LINAC voltage using a radiation field of 10 × 10 cm and SSD 100 cm is shown in Fig. 6. Fig. 7 shows that the voltage increases the position to reach 100% of the dose gets deeper. The X-rays produced by the LINAC device at voltages of 6, 10, and 18 MV have similar dose profiles. The dose profile tends to decrease as it approaches the edge of the irradiation field. This decrease is due to the penumbra effect [27]. A penumbra

region appears because of X-ray radiation exposure in the radiation field that is limited by the collimator jaws [30][31].

Simulation of dose profile at the voltage of 6, 10, and 18 MV provides different relative doses at 5, 10 and 20 cm depth. At 6 MV, the relative dose at the depth of 5, 10 and 20 cm are respectively 41.5%, 62.2% and 80.1%. At 10 MV, they are 42.2%, 66.7% and 83.4%. At 18 MV, highest values of relative dose are obtained, i.e., 45%, 66.3% and 85.0%. It shows that as the voltage of LINAC increases, the ability of X-ray radiation to penetrate the water phantom correspondingly increases. The increase in penetrating power is due to an increase in the energy of the x-rays [32][33].

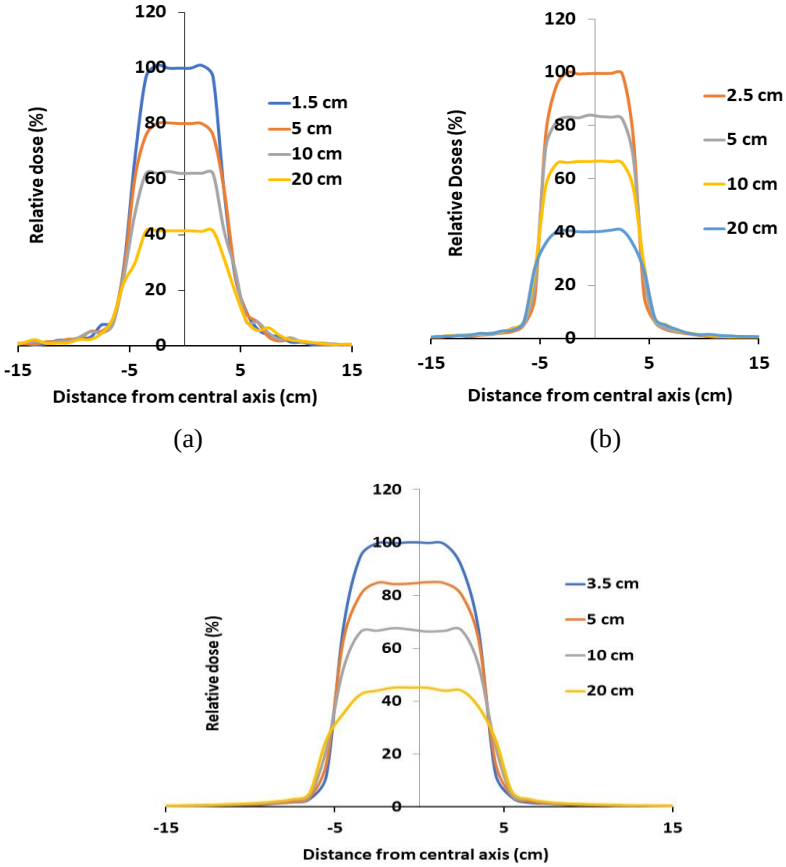

Fig. 7. Dose profile curve produced by LINAC at working voltage of (a) 6 MV (b) 10 MV (c) 18 MV

The degree of uniformity of the photon beam produced by the LINAC machine can be determined from the flatness value of the X-ray beam. The flatness value at the voltage of 6, 10, and 18 MV calculated at a depth of 10 cm is shown in Table 2. The flatness values of the X-ray photon beam are all less than 2%. They are below the permissible flatness value, which is < 2% [34][35]. However, the dose profile still shows a dose profile that is not symmetrical, as shown in Fig. 6. The area of the left side is not the same as that of the right side. It suggests that the X-ray beams striking the water phantom have different intensities. The difference in intensity is caused by the presence of contaminants in the form of secondary electrons and neutrons that arise when the primary electrons interact with the target [36][37]. The two beams spread out following the X-ray photons. The use of an ion chamber and layered flattening filter is deemed responsible for reducing these contaminants so that the generated X-rays increase the uniformity of the beam [38]−[40].

Table 2. Flatness percentage of a radiation beam

No	Linac (MV)	Percentage of deviation from flatness (%)
1	6	1.6
2	10	1.9
3	18	1.2

4. CONCLUSION

The modeling of the LINAC therapy machine based on the Siemen Primus LINAC device has been successfully carried out. The modeling of the LINAC therapy device agrees with the actual X-ray apparatus. The model of the X-ray therapy device has produced X-ray traces and their spectrum. The calculation of Percentage Depth Dose (PDD) with a radiation field of 10×10 cm^2 at the working voltage of 6, 10, and 18 MV results in maximum doses at a depth of, respectively, 1.5 cm, 2.5 cm, and 3.5 cm. Based on the analysis of the PDD curve, the value of the build-up factor for each LINAC voltage agrees with the reference. The radiation dose profile with a radiation field of 10×10 cm^2 demonstrates that the flatness of the dose profile occurs at the depth of 20 cm with a percentage value of flatness at 1.6%, 1.9%, and 1.2%. The result satisfies the stipulated tolerance limit of < 2 %. For future research, it is necessary to improve the model by adding an ion chamber and a layered flattening filter to the LINAC head component so that the X-ray beam produced is more uniform.

REFERENCES

[1] B. J. Healy, D. van der Merwe, K. E. Christaki, and A. Meghzifene, "Cobalt-60 Machines and Medical Linear Accelerators: Competing Technologies for External Beam Radiotherapy," *Clin. Oncol*., vol. 29, no. 2, pp. 110–115, 2017, https://doi.org/10.1016/j.clon.2016.11.002

[2] S. Corradini, F. Alongi, N. Andratschke, C. Belka, L. Boldrini, F. Cellini, and M. Niyazi, "MR-guidance in clinical reality: Current treatment challenges and future perspectives," *Radiat. Oncol.*, vol. 14, no. 1, pp. 1–12, 2019, https://doi.org/10.1186/s13014-019-1308-y

[3] T. Tuğrul and O. Eroğul, "Determination of initial electron parameters by means of Monte Carlo simulations for the Siemens Artiste Linac 6 MV photon beam," *Reports Pract. Oncol. Radiother*., vol. 24, no. 4, pp. 331–337, 2019, https://doi.org/10.1016/j.rpor.2019.05.002.

[4] T. C. F. Fonseca,. B. M. Mendes, M. A. D. S. Lacerda, L. A. C. Silva., L. Paixão, F. M. Bastos, and J. P. R. Junior, "MCMEG: Simulations of both PDD and TPR for 6 MV LINAC photon beam using different MC codes," *Radiat. Phys. Chem.*, vol. 140, pp. 386–391, 2017, https://doi.org/10.1016/j.radphyschem.2017.03.048.

[5] M. R. Bayatiani, F. Fallahi, A. Aliasgharzadeh, M. Ghorbani, B. Khajetash, and F. Seif, "A comparison of symmetry and flatness measurements in small electron fields by different dosimeters in electron beam radiotherapy," *Reports Pract. Oncol. Radiother*., vol. 26, no. 1, pp. 50–58, 2021, https://doi.org/10.5603/RPOR.a2021.0009.

[6] J. Kim, D. O, Shin, S. H. Choi, S. Min, N. Kwon, U. Jung, and D. W. Kim, "Guideline on Acceptance Test and Commissioning of High-Precision External Radiation Therapy Equipment," *Prog. Med. Phys*., vol. 29, no. 4, p. 123, 2018, https://doi.org/10.14316/pmp.2018.29.4.123.

[7] B. Faddegon, J. Ramos-Méndez, J. Schuemann, A. McNamara, J. Shin, , J. Perl, and H. Paganetti, "The TOPAS tool for particle simulation, a Monte Carlo simulation tool for physics, biology and clinical research," *Phys. Medica*, vol. 72, no. 4, pp. 114–121, 2020, https://doi.org/10.1016/j.ejmp.2020.03.019

[8] T. Gray, N. Bassiri, N. Kirby, S. Stathakis, and K. M. Mayer, "Implementation of a simple clinical linear accelerator beam model in MCNP6 and comparison with measured beam characteristics," *Appl. Radiat. Isot.*, vol. 155, 2020, https://doi.org/10.1016/j.apradiso.2019.108925

[9] J. Fiak, M., Fathi, A., Inchaouh, "Monte Carlo Simulation of a 18 MV Medical Linac Photon Beam Using GATE/GEANT4," *Moscow Univ. Phys*, vol. 76, pp. 15–21, 2021, https://doi.org/10.3103/S0027134921010069

[10] M. Asai, M. A. Cortés-Giraldo, V. Giménez-Alventosa, V. Giménez Gómez, and F. Salvat, "The PENELOPE Physics Models and Transport Mechanics. Implementation into Geant4," *Front. Phys*., vol. 9, no. 12, pp. 1–20, 2021, https://doi.org/10.3389/fphy.2021.738735.

[11] T. Furuta and T. Sato, "Medical application of particle and heavy ion transport code system PHITS," *Radiol. Phys. Technol*., vol. 14, no. 3, pp. 215–225, 2021, https://doi.org/10.1007/s12194-021-00628-0.

[12] T. Sato, Y. Iwamoto, S. Hashimoto, T. Ogawa, T. Furuta, S.I. Abe, and K. Niita, "Features of Particle and Heavy Ion Transport code System (PHITS) version 3.02," *J. Nucl. Sci. Technol*., vol. 55, no. 6, pp. 684–690, 2018, https://doi.org/10.1080/00223131.2017.1419890.

[13] M. Ghorbani, M. Azizi, B. Azadegan, A. A. Mowlavi, Z. A. Rahvar, and W. Wagner, "Dosimetric evaluation of neutron contamination caused by dental restorations during photon radiotherapy with a 15 MV Siemens Primus linear accelerator," *Radiat. Phys. Chem*., vol. 174, no. 7, 2019, p. 108961, 2020, https://doi.org/10.1016/j.radphyschem.2020.108961.

[14] R. H. Hasan, S. I. Essa, and M. A. AL-Naqqash, "Depth dose measurement in water phantom for two X-ray energies (6 MeV and 10 MeV) in comparison with actual planning," *Iraqi J. Sci*., vol. 60, no. 8, pp. 1689–1693, 2019, https://doi.org/10.24996/ijs.2019.60.8.5.

[15] W.M.Abou-TalebaM.H.HassanbE.A.El_MallahcS.M.Kotba, "MCNP5 evaluation of photoneutron production from the Alexandria University 15 MV Elekta Precise medical LINAC," *Appl. Radiat. Isot*., vol. 135, no. 5, pp. 184–191, 2018, https://doi.org/10.1016/j.apradiso.2018.01.036

[16] M. G. Ahad Ollah Ezzati, Matthew T. Studenski, "Spatial mesh-based surface source model for the electron contamination of an 18 MV photon beams," *J. Med. Phys*., vol. 45, no. 4, pp. 221–225, 2020, https://doi.org/10.4103/jmp.JMP_29_20.

[17] W. B. Nurdin, A. Purnomo, and S. Dewang, "Source to Skin Distance (SSD) Characteristics from Varian CX Linear

Accelerator," *J. Phys. Conf. Ser.*, vol. 979, no. 1, pp. 1–5, 2018, https://doi.org/10.1088/1742-6596/979/1/012076.
[18] G. Martin-Martin, S. Walter, and E. Guibelalde, "Dosimetric impact of failing to apply correction factors to ion recombination in percentage depth dose measurements and the volume-averaging effect in flattening filter-free beams," *Phys. Medica*, vol. 77, no. 8, pp. 176–180, 2020, https://doi.org/10.1016/j.ejmp.2020.07.006.
[19] M. Hossain and J. Rhoades, "On beam quality and flatness of radiotherapy megavoltage photon beams," *Australas. Phys. Eng. Sci. Med.*, vol. 39, no. 1, pp. 135–145, 2016, https://doi.org/10.1007/s13246-015-0408-8.
[20] C. M. Ma, I. J. Chetty, J. Deng, B. Faddegon, S. B. Jiang, J. Li, and E. Traneus, "Beam modeling and beam model commissioning for Monte Carlo dose calculation-based radiation therapy treatment planning: Report of AAPM Task Group 157," *Med. Phys.*, vol. 47, no. 1, pp. 1–18, 2020, https://doi.org/10.1002/mp.13898.
[21] S. Vichi, D. Dean, S. Ricci, F. Zagni, P. Berardi, and D. Mostacci, "Activation study of a 15MeV LINAC via Monte Carlo simulations," *Radiat. Phys. Chem.*, vol. 172, no. 7, p. 108758, 2020, https://doi.org/10.1016/j.radphyschem.2020.108758.
[22] P. Buaphad, Y. Kim, K. Song, H. Dal Park, C. Kim, S. Lee, and J. Ju, "X-ray dose rate estimation model for an electron linac with thick tungsten target," *Nucl. Instruments Methods Phys. Res. Sect. B Beam Interact. with Mater. Atoms*, vol. 498, no. 4, pp. 61–67, 2021, https://doi.org/10.1016/j.nimb.2021.04.009.
[23] T. Almatani, "Validation of a 10 MV photon beam Elekta Synergy linear accelerator using the BEAMnrc MC code," *J. King Saud Univ. - Sci.*, vol. 33, no. 4, p. 101406, 2021, https://doi.org/10.1016/j.jksus.2021.101406.
[24] J. S. E. Jiménez, M. D. Lagos, and S. A. Martinez-Ovalle, "A Monte Carlo Study of the Photon Spectrum due to the Different Materials Used in the Construction of Flattening Filters of LINAC," *Comput. Math. Methods Med.*,, 2017, https://doi.org/10.1155/2017/3621631.
[25] A. Baumgartner, A. Steurer, and F. Josef Maringer, "Simulation of photon energy spectra from Varian 2100C and 2300C/D Linacs: Simplified estimates with PENELOPE Monte Carlo models," *Appl. Radiat. Isot.*, vol. 67, no. 11, pp. 2007–2012, 2009, https://doi.org/10.1016/j.apradiso.2009.07.010.
[26] D. E. Krim, D. Bakari, M. Zerfaoui, A. Rrhioua, and Y. Oulhouq, "Monte Carlo evaluation of particle interactions within the patient-dependent part of Elekta 6 MV photon beam applying IAEA phase space data," *Reports Pract. Oncol. Radiother.*, vol. 26, no. 6, pp. 928–938, 2021, https://doi.org/10.5603/RPOR.a2021.0111.
[27] C. Anam, D.S. Soejoko, F. Haryanto, S. Yani, and G. Dougherty, "Electron contamination for 6 MV photon beams from an Elekta linac: Monte Carlo simulation," *J. Phys. Its Appl.*, vol. 2, no. 2, pp. 97–101, 2020, https://doi.org/10.14710/jpa.v2i2.7771.
[28] Y. Li, Y.Gao, X. Liu, J. Shi, J. Xia, J. Yang, and L. Mao, "The influence of beam delivery uncertainty on dose uniformity and penumbra for pencil beam scanning in carbon-ion radiotherapy," *PLoS One*, vol. 16, no. 4, pp. 1–18, 2021, https://doi.org/10.1371/journal.pone.0249452.
[29] A. Das and T. Singha, "Development of a new Monte Carlo based transport code to calculate photon exposure build-up factors in various shielding arrangements," *Radiat. Phys. Chem.*, vol. 194, no. 5, pp. 11–28, 2022, https://doi.org/10.1016/j.radphyschem.2022.110028.
[30] S. Farrukh, N. Ilyas, M. Naveed, A. Haseeb, M. Bilal, and J. Iqbal, "Penumbral Dose Characteristics of Physical and Virtual Wedge Profiles," *Int. J. Med. Physics, Clin. Eng. Radiat. Oncol.*, vol. 6, no. 2, pp. 216–224, 2017, https://doi.org/10.4236/ijmpcero.2017.62020.
[31] N. Qomariyah, R. Wirawan, L. Mardiana, and K. Al Hadi, "Distributions dose analysis for 6 MV photon beams using Monte Carlo-GEANT4 simulation," *AIP Conf. Proc.*, vol. 2169, no. 11, pp. 1–6, 2019, https://doi.org/10.1063/1.5132656.
[32] N. Khaledi, M. Dabaghi, D. Sardari, F. Samiei, F. G. Ahmadabad, G. Jahanfarnia, and X. Wang, "Investigation of photoneutron production by Siemens artiste linac: A Monte Carlo Study," *Radiat. Phys. Chem.*, vol. 153, pp. 98–103, 2018, https://doi.org/10.1016/j.radphyschem.2018.06.006.
[33] H. Do Huh and S. Kim, "History of Radiation Therapy Technology," *Prog. Med. Phys.*, vol. 31, no. 3, pp. 124–134, 2020, https://doi.org/10.14316/pmp.2020.31.3.124.
[34] E. Hoseinnezhad, G. Geraily, M. Esfahani, M. Farzin, and S. Gholami, "Comparison of calculated and measured basic dosimetric parameters for total body irradiation with 6- And 18-MV photon beams," *J. Radiother. Pract.*, vol. 20, no. 1, pp. 66–70, 2021, https://doi.org/10.1017/S1460396919001067.
[35] Bn. M. Sümeyra Cana, and Didem Karaçetin, "Beam modeling and commissioning for Monte Carlo photon beam on an Elekta Versa HD LINAC," *Appl. Radiat. Isot.*, vol. 180, no. 1, pp. 11–54, 2022, https://doi.org/10.1016/j.apradiso.2021.110054.
[36] D. Dawn, S. Pal, R. Bakshi, A. K. Kinhikar, R. A. Joshi, K. Jamema, S. V. Datta, "Evaluation of in-field Evaluation of in-field neutron production for medical LINACs with and without flattening filter for various beam parameters - Experiment and Monte Carlo simulation," *Comput. Math. Methods Med.*, vol. 118, no. 11, pp. 98–107, 2018, https://doi.org/10.1016/j.radmeas.2018.04.005
[37] V. Gracanin, S. Guatelli, D. Cutajar, I. Cornelius, L. T. Tran, D. Bolst, and A. Rosenfeld, "A convenient verification method of the entrance photo-neutron dose for an 18 MV medical linac using silicon p-i-n diodes," *Radiat. Meas.*, vol. 106, no. 2, pp. 391–398, 2017, https://doi.org/10.1016/j.radmeas.2017.01.004.
[38] A. J. Cetnar and D. J. DiCostanzo, "The lifetime of a linac monitor unit ion chamber," *J. Appl. Clin. Med. Phys.*, vol. 22, no. 12, pp. 108–114, 2021, https://doi.org/10.1002/acm2.13463.
[39] A. Zeghari, R. Saaidi, and C. E. M. R, "Linac with Free Flattening Filter Mode," *J Biomed Phys Eng.*, vol. 444, no. 4, pp. 437–444, 2019, https://doi.org/10.31661/jbpe.v0i0.924.
[40] S. Bajwa, A. Gul, S. Ahmed, and M. B. Kakakhel, "Monte Carlo commissioning of radiotherapy LINAC—

Introducing an improved methodology," *Reports Pract. Oncol. Radiother*., vol. 25, no. 5, pp. 720–724, 2020, https://doi.org/10.1016/j.rpor.2020.06.009.

BIOGRAPHY OF AUTHORS

Bilalodin received his bachelor degree in Physics from Department of Physics, Universitas Diponegoro, Indonesia, in 1993 and master degree from Physics Department, Institute Teknologi Bandung (ITB), Indonesia, in 2000. Doctoral degree in physics obtained from Universitas Gadjah Mada, in 2000. Current research interest is modeling of therapeutic particles in Medical Physics. Email: bilalodin@unsoed.ac.id

Farzand Abdullatif received his bachelor degree in Physics from Department of Physics, Institut Teknologi Bandung in 1995 and master degree from the same department in 2000. He was awarded doctoral degree from The Australian National University in 2017. His research interest includes Medical Physics and Fluid Dynamics. Email: farzand@unsoed.ac.id